

## Electronic Supplementary Information

### Hierarchical FeTiO<sub>3</sub>-TiO<sub>2</sub> hollow spheres for efficient simulated sunlight-driven water oxidation

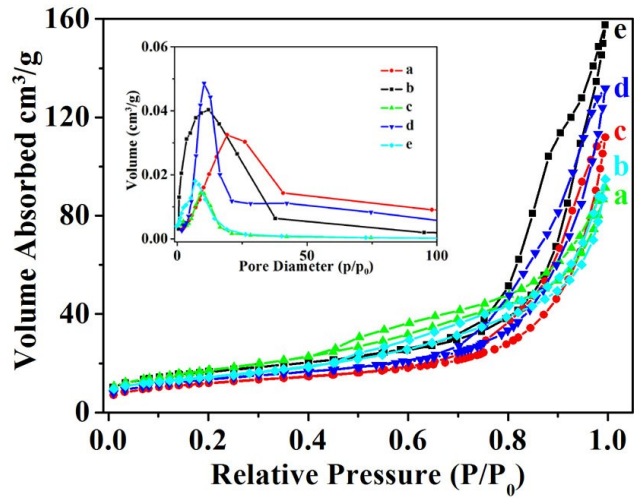
Taoran Han,<sup>a</sup> Yajie Chen,<sup>a</sup> Guohui Tian,<sup>\*a,b</sup> Jian-Qiang Wang,<sup>c</sup> Zhiyu Ren,<sup>a</sup> Wei Zhou<sup>a</sup> and Honggang Fu<sup>\*a</sup>

<sup>a</sup> Key Laboratory of Functional Inorganic Material Chemistry, Ministry of Education of the People's Republic of China, Heilongjiang University, Harbin 150080 P. R. China

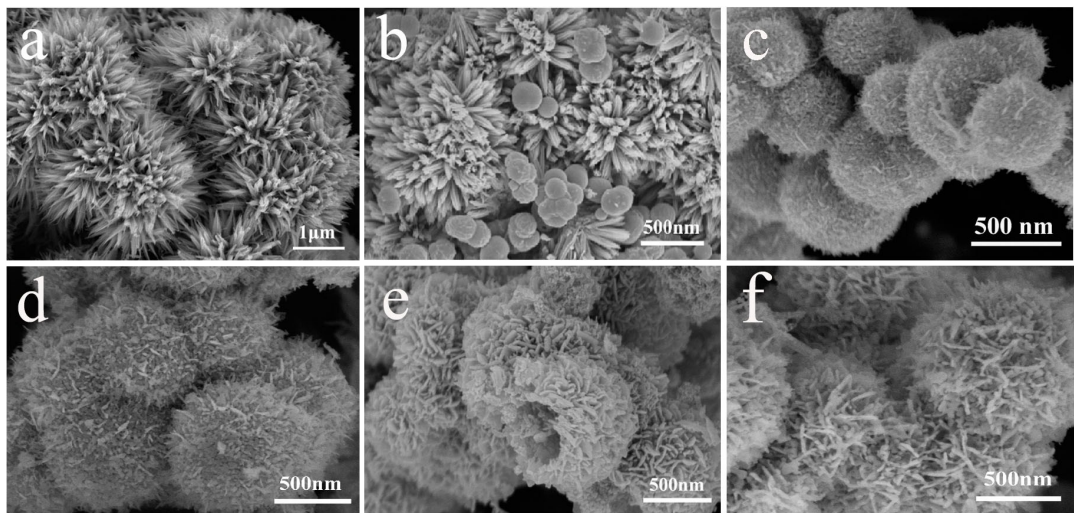
<sup>b</sup> Key Laboratory of Chemical Engineering Process & Technology for High-efficiency Conversion, College of Heilongjiang Province, School of Chemistry and Materials Science, Heilongjiang University, Harbin 150080, China.

<sup>c</sup> Shanghai Synchrotron Radiation Facility (SSRF), Shanghai Institute of Applied Physics, Chinese Academy of Sciences, Shanghai 201204, P. R. China

Corresponding author E-mail: tiangh@hlju.edu.cn; fuhg@vip.sina.com, Tel.: +86 451 8660 4330, Fax: +86 451 8667 3647



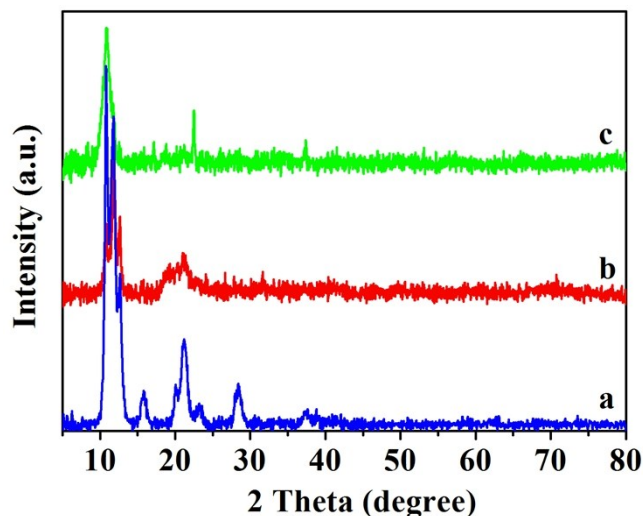
**Fig. S1** N<sub>2</sub> adsorption-desorption isotherms curves of the different samples, (a) TiO<sub>2</sub>, (b) FeTiO<sub>3</sub>-TiO<sub>2</sub> (Ti:Fe=1:0.25), (c) FeTiO<sub>3</sub>-TiO<sub>2</sub> (Ti:Fe=1:0.5, (d) FeTiO<sub>3</sub> (e) FeTiO<sub>3</sub>-TiO<sub>2</sub> (Ti:Fe=1:0.75).



**Fig. S2** SEM image obtained precursors prepared from the first solvothermal reaction, (a) SEM images showing the morphological evolution of the obtained precursors prepared from the second solvothermal reaction with different reaction time, (b) 0.5 h, (c) 3 h, (d) 6 h, (e) 9 h, (f) 12 h.

**Table S1.** BET surface area of the prepared different samples

Samples	TiO <sub>2</sub>	FeTiO <sub>3</sub> -TiO <sub>2</sub> (Ti:Fe=1:0.25)	FeTiO <sub>3</sub> -TiO <sub>2</sub> (Ti:Fe=1:0.50)	FeTiO <sub>3</sub> -TiO <sub>2</sub> (Ti:Fe=1:0.75)	FeTiO <sub>3</sub> (Ti:Fe=1:1)
Surface area(m <sup>2</sup> g <sup>-1</sup> )	48.8	45.4	51.51	63.26	58.45



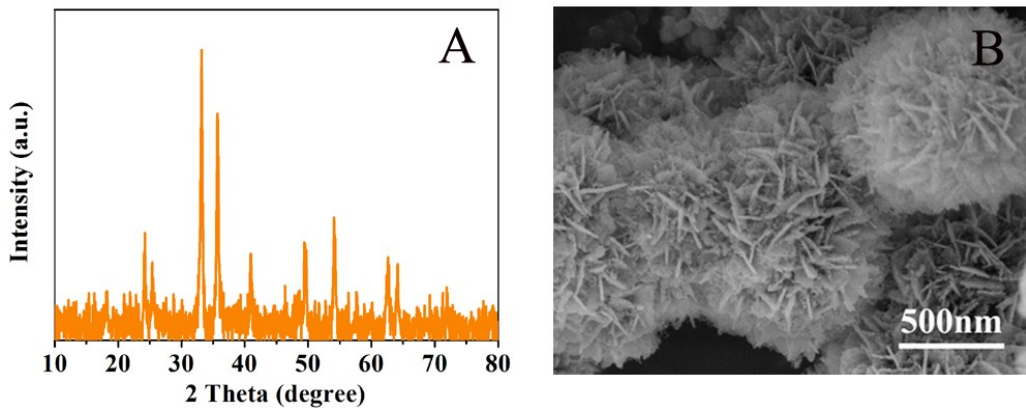
**Fig. S3** XRD patterns of the prepared precursors of (a) TiO<sub>2</sub>, (b) FeTiO<sub>3</sub>-TiO<sub>2</sub> (Ti:Fe=1:0.75), and (c) FeTiO<sub>3</sub>.

Table S2. Fit parameters of the EXAFS spectra for FeTiO<sub>3</sub>, TiO<sub>2</sub> and FeTiO<sub>3</sub>-TiO<sub>2</sub>.

<b>Sample</b>	<b>shell</b>	<b>N<sup>[a]</sup></b>	<b>R<sup>[b]</sup></b>	<b>σ<sup>2</sup> (10<sup>-3</sup> Å<sup>2</sup>)<sup>[c]</sup></b>	<b>Δ E<sub>0</sub> (eV)<sup>[d]</sup></b>
FeTiO <sub>3</sub>	Fe-O	3	1.92 ± 0.01	6.0 ± 1.0	-5.7
	Fe-O	3	2.05 ± 0.01	12.6 ± 3.4	-5.7
	Fe-Fe/Ti	4	3.00 ± 0.01	11.5 ± 1.1	-3.0
FeTiO <sub>3</sub> -TiO <sub>2</sub>	Fe-O	3	1.92 ± 0.01	7.0 ± 1.0	-5.7
	Fe-O	3	2.04 ± 0.01	11.0 ± 2.6	-5.7
	Fe-Fe/Ti	5.3 ± 1.5	3.01 ± 0.01	15.4 ± 3.3	-3.0
FeTiO <sub>3</sub> -TiO <sub>2</sub>	Ti-O	5.3 ± 0.7	1.96 ± 0.01	5.2 ± 1.2	-0.9
	Ti-Ti	2	3.01 ± 0.01	3.4 ± 1.3	-10.3
	Ti-O	4	3.54 ± 0.04	5.0 ± 5.0	-0.9
FeTiO <sub>3</sub>	Ti-Ti	4	3.85 ± 0.02	7.5 ± 3.2	-10.3
	Ti-O	6	1.95 ± 0.01	9.4 ± 0.7	-2.8
	Ti-Fe/O	3	3.09 ± 0.02	11.0 ± 2.1	-2.8
	Ti-O/Fe	5	3.75 ± 0.05	8.2 ± 7.8	-2.8

[a] Coordination number; [b] Distance between absorber and backscatterer atoms; [c] Debye-Waller factor; [d] Inner potential correction.

The X-ray absorption data at the Ti L<sub>3</sub> - edge and Fe L<sub>3</sub> - edge of the samples were recorded at room temperature in transmission mode using ion chambers or in the fluorescent mode with silicon drift fluorescence detector at beam line BL14W1 of the Shanghai Synchrotron Radiation Facility (SSRF), China. The station was operated with a Si(111) double crystal monochromator. During the measurement, the synchrotron was operated at energy of 3.5 GeV and a current between 150-210 mA. Energy calibrations were calibrated by measuring Fe and Ti metal foil standards, assigning the first inflection point to 7112 eV and 4966 eV, respectively. All fits to the EXAFS data were performed using the program ARTEMIS.30.



**Fig. S4** X-ray diffraction pattern (A) and SEM image (B) after the catalytic reaction of hierarchical FeTiO<sub>3</sub>-TiO<sub>2</sub> composite hollow spheres.

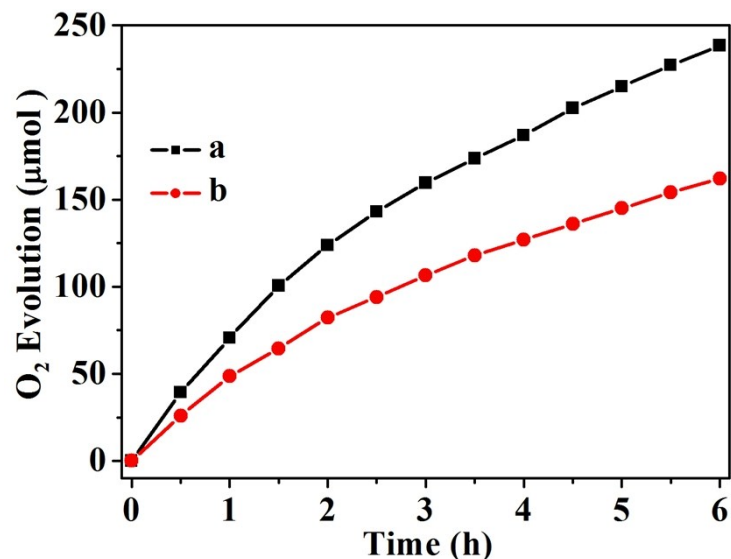


**Fig. S5** Comparision of the oxygen evolution of the hierarchical FeTiO<sub>3</sub>-TiO<sub>2</sub> composite hollow spheres (Ti:Fe=1:0.75) (a), and the corresponding crushed one (b) under simulated sunlight (AM 1.5).

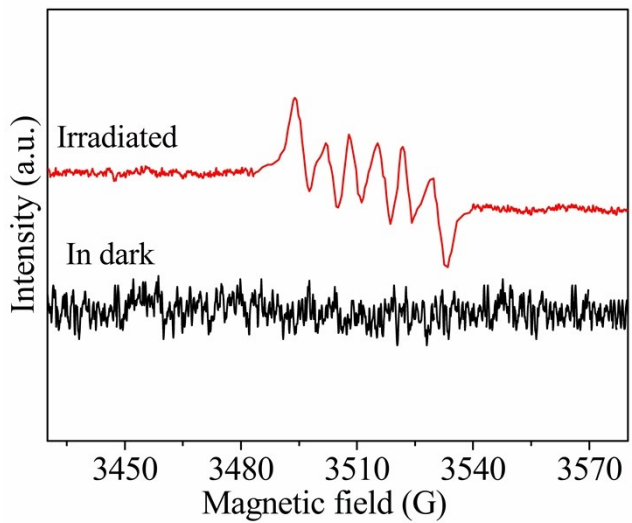


**Fig. S6** DMPO spin-trapping ESR spectra recorded at ambient temperature with hierarchical FeTiO<sub>3</sub>-TiO<sub>2</sub> hollow spheres in methanol dispersion (for DMPO-•O<sup>2-</sup>) under visible-light irradiation ( $\lambda > 400$  nm).

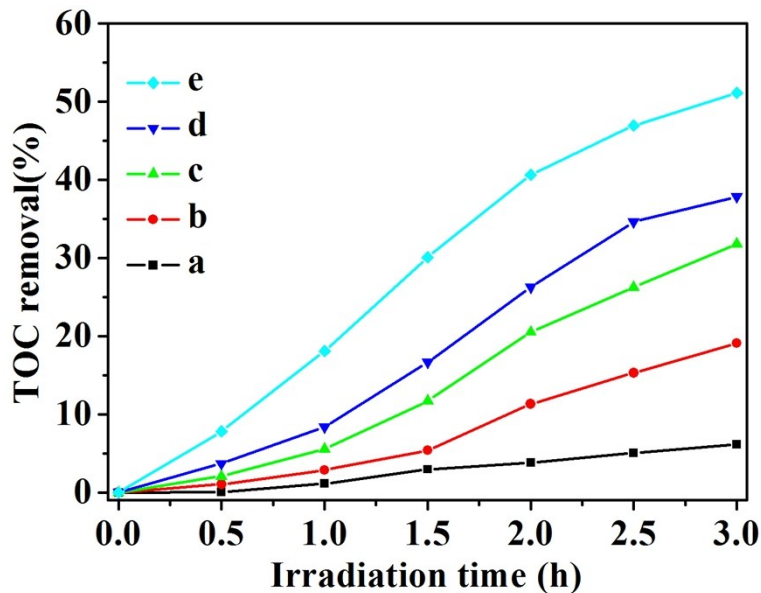


**Fig. S7** The removal of TOC during the 2, 4-dichlorophenol photodegradation process in different aqueous dispersions under visible light irradiation: (a) TiO<sub>2</sub>, (b) FeTiO<sub>3</sub>-TiO<sub>2</sub> (Ti:Fe=1:0.25), (c) FeTiO<sub>3</sub>-TiO<sub>2</sub> (Ti:Fe=1:0.5), (d) FeTiO<sub>3</sub> (e) FeTiO<sub>3</sub>-TiO<sub>2</sub> (Ti:Fe=1:0.75).